International Journal of Nanoelectronics and Materials
Volume 15 (Special Issue) March 2022 [183-207]

Electrospinning of Polyacrylonitrile Nanofibres and Applications in Membrane Distillation Technology: A Review

M. W. Azmil Arif[1], A. H. Nurfaizey[1,2]*, M. A. Salim[1,2], N. A. Masripan[1,2], J. Jaafar[3] and M. H. D. Othman[3]

[1]Fakulti Kejuruteraan Mekanikal, Universiti Teknikal Malaysia Melaka,
Hang Tuah Jaya, 76100 Durian Tunggal, Melaka, Malaysia
[2]Centre for Advanced Research on Energy, Universiti Teknikal Malaysia Melaka,
Hang Tuah Jaya, 76100 Durian Tunggal, Melaka, Malaysia
[3]Advanced Membrane Technology Research Centre (AMTEC), Universiti Teknologi Malaysia,
81310 Skudai, Johor, Malaysia

ABSTRACT

Water scarcity is a major concern in some parts of the world today. In some countries, seawater desalination through membrane distillation (MD) has been employed to overcome the crisis. However, there are two primary challenges hindering the effectiveness of the MD process, which are vapour flux declination and membrane wetting. Recently, electrospun fibres have been proposed as an alternative technique to develop novel membrane modules for the MD process. In this regard, polyacrylonitrile (PAN) in the form of electrospun fibres is a popular choice due to its superior characteristics such as hydrophobic surface, small fibre diameter, low thermal conductivity, and good mechanical strength. However, it is dependent on the fabrication method, which has a significant impact on the characteristics of the final products. Electrospinning is the most efficient technique for producing polymeric electrospun fibres utilising electrical charges. Although electrospinning is frequently seen as a simple process, it involves a number of complex processing parameters that must be optimised in order to produce high-quality fibre membranes. In this review, a brief overview is presented on the electrospinning of PAN electrospun fibres, as well as the range of optimum processing parameters. This review also focuses on the properties of PAN electrospun fibres and current fabrication methods for developing membrane modules for the MD system.

Keywords: Electrospinning, polyacrylonitrile, membrane distillation, nanofibres

1. INTRODUCTION

Clean water resources play an important role in the source of life, including economic, social, and environmental. As of today, it remains a major problem where it is estimated that by 2030, almost half of the world's population will be facing a lack of access to clean water sources, especially in water-stressed regions, such as in eastern China, India, US, Europe and some parts of Australia [1, 2]. In the worst-case scenario, this water crisis could worsen over time due to climate change, ineffective water management, and excessive or misuse of freshwater resources [3]. Thus, in order to meet the increasing demand for clean water, membrane distillation (MD) has emerged as an alternative and viable option for the water purification process, particularly in near-sea regions [4]. MD is known as the most promising technology in treating saline and contaminated water, where it has the ability to treat high salinity feedwater by only using a small amount of heat and operating at low temperatures [5–7].

In the MD system, waterproof or microporous membrane typically made from hydrophobic materials is used as a physical barrier between the hot feed-side and cold-permeate side, which filters all non-volatile solutes and only allow pure water vapour (freshwater) to pass through the membrane pores [8–10] (Figure 1). Despite having a high salt rejection efficiency, MD has two major drawbacks: i.e. vapour flux declination and membrane wetting [11,12]. Vapour flux declination (also known as membrane fouling) occurs when particulate matter accumulates on the hydrophobic membrane's surface or within membrane pores, impeding the vapour transmission process. [13]. Meanwhile, membrane wetting occurs when the membrane cannot withstand hydraulic pressure, which means that the operating pressure exceeds the liquid entry pressure (LEP) [14]. Hence, the feed solution leaks through the membrane pores and contaminates the permeate side [15]. In addition, the changes of surface behaviour from hydrophobic to hydrophilic also could lead to fouling deposition and pore wetting [16].

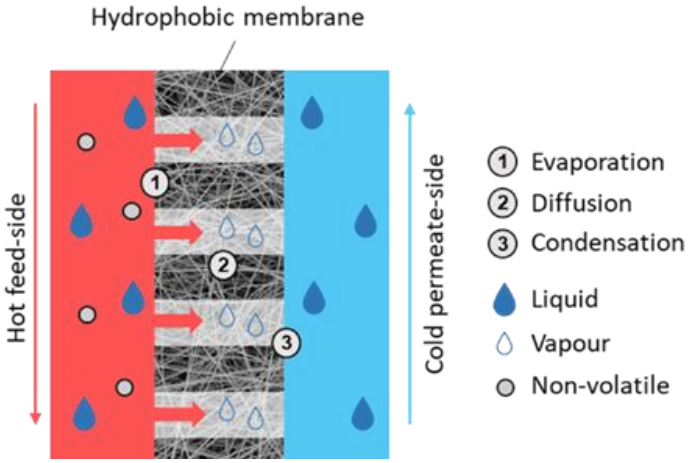

Figure 1. Schematic diagram of membrane distillation process.

In order to resolve the above-mentioned issues, polymeric nanofibre coatings have been proposed as they have prodigious characteristics such as lightweight, small diameters, controllable pore structures, and high surface-area-to-volume ratios [17–19]. To date, various types of polymers have been proposed, such as polydimethylsiloxane (PDMS), polyacrylonitrile (PAN), polyvinyl alcohol (PVA), polyvinylidene fluoride (PVDF), and polypropylene (PP) [20,21]. Among these polymers, polyacrylonitrile (PAN) is one of the most frequently used in the fabrication of MD membranes due to its hydrophobic properties, good thermal stability, solvent resistance, and high mechanical strength [22–24]. Moreover, numerous PAN-based membranes have been developed using a variety of physical and chemical treatments to enhance their ability to remove bacteria, dyes, and metal ions from seawater or wastewater [25–27]. For instance, Wu *et al.,* [28] altered the characteristics of PAN-based membranes with carbon tetrafluoride (CF_4) plasma treatment and PDMS surface coating. The performance of the modified PAN membrane was found to be highly effective at removing ethyl acetate (EtAc) from wastewater.

Furthermore, membrane hydrophobisation is an effective method for resolving the wetting issue in the MD process [29]. Fang *et al.,* [30] discovered that the surface wettability of PAN nanofibres could be increased by coating them with silica nanoparticles solutions and Tridecafluorooctyltriethoxysilane (FAS), where the treated PAN nanofibre membranes formed a superhydrophobic surface with a contact angle as high as 157.1°. Apart from that, Liu *et al.,* [31] also used the same approach by coating PAN nanofibres membrane with 1H, 1H, 2H, 2H-Perfluorodecyl methacrylate followed with plasma treatment. The modified membrane demonstrated a steady vapour flux (59.42 kg m^{-2} h^{-1}) and a significant increase in salt rejection efficiency (99.93%). On the other hand, when developing a membrane module, researchers must take into account both the advantages and disadvantages of the chosen approach. For instance,

Ebrahimi *et al.,* [32] coated the flat sheet membrane with TiO_2 nanoparticles and 1H,1H,2H,2H-Perfluorododecyl trichlorosilane (FTCS) to enhance surface wettability properties. As a result, even though the modified membrane had a high contact angle (174°), the vapour flux obtained was only 2.3 kg m^{-2} h^{-1}. Thus, the pursuit of efficient methods for fabricating high-performance membranes has stimulated ongoing research and development.

Currently, there are several methods and techniques have been introduced for the preparation of MD membranes, including self-assembly, template synthesis, melt blowing, electrospinning, and phase separation [33,34]. In particular, electrospinning is the most straightforward and cost-effective method for producing fine polymeric fibrous materials and has been widely used in industrial applications and academic research [35–38]. According to Essalhi *et al.,* [39], nanofibres membranes produced via electrospinning typically have a hydrophobic surface, small pore structures and high porosity. The electrospinning technique consists of five main process parameters, which are solution concentration, applied voltage, the distance between needle-tip to the grounded collector, polymer flow rate, and ambient temperature [40,41]. Numerous studies related to electrospinning process parameters have been conducted previously. However, contradictory findings have also been reported regarding the effects of these parameters on the quality of fibre production, particularly when dealing with different solute and solvent systems [42]. Hence, optimising electrospinning parameters is important as it could significantly affect the behaviour of the nanofibre membranes and MD performance [43].

The tremendous number of publications relating to MD and electrospun nanofibres published in scientific journals has accelerated the development of desalination technologies. However, to the best of the author's knowledge, very few of the published works focused on the potential of PAN electrospun fibres in the development of MD membranes. Hence, in this review, a brief overview is presented on the electrospinning process, as well as the range of optimum processing parameters. This review also focuses on the critical characteristics of PAN electrospun fibre and its current application in membrane distillation technology.

2. THE ELECTROSPINNING PROCESS

Electrospinning is a technique for producing fibres that operate using high electrical charges that will create a stream of ultra-fine fibres. This technique was invented in 1934, most notably through a series of inventions by Anton Formhals [44]. However, this technique was less popular in the earlier years due to technological limitations and a lack of knowledge about the advantages of nanoscale materials [44]. In the early 1990s, with the help of advanced technology, groups of researchers managed to develop a simple and powerful technique that was capable of producing polymeric fibres with average fibre diameter in the range of nanometre to micrometre [45]. A basic electrospinning machine is typically composed of four major components: (i) a grounded collector electrode, (ii) a needle tip with a small orifice (spinneret), (iii) a polymer solution supply, and (iv) a high-voltage power supply, as shown in Figure 2 [46].

The electrospinning process starts when an optimum applied voltage is applied on the tip of a spinneret that will trigger a polymer jet formation at the vertex of the conical-shaped droplet, also known as Taylor cone [47–49]. At this threshold voltage and beyond, strong electrostatic repulsive forces within the polymer will overcome the surface tension of the polymer droplet. Thus, the polymer solution will be ejected from the spinneret and stretched longitudinally in the direction of electric fields and then travel towards the grounded collector electrode. After a certain moment, the electrostatic repulsive forces weaken, and the charged jet polymer's motion becomes unstable, resulting in the formation of a whipping instability [50,51]. Therefore, an enormous mechanical stretching is formed, resulting in thinning the fibres as the remaining solvent in the polymer jet continues to evaporate and finally lands on the grounded collector as dry fibre webs.

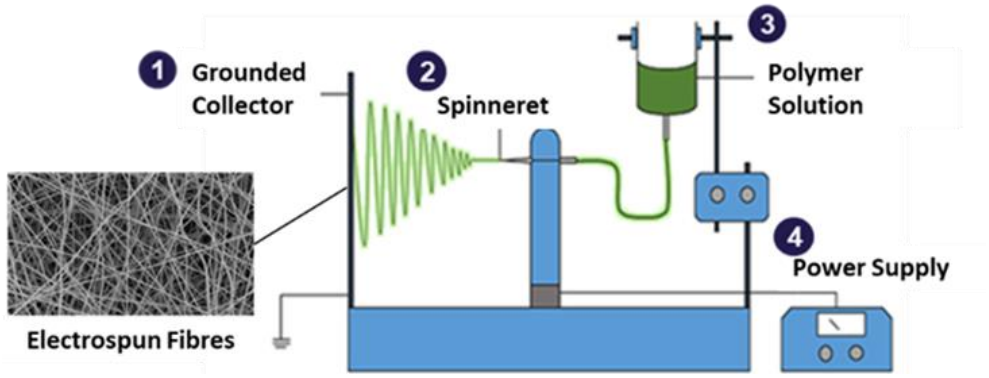

Figure 2. Schematic diagram of a typical electrospinning machine.

3. ELECTROSPINNING PROCESS PARAMETERS

3.1 Solution Concentration

Concentration is the amount of solute that has been dissolved in a particular amount of solvent. Typically, most researchers used the terms volume per volume (% v/v), weight percentage (wt %), or weight per volume (% w/v) in describing a solution concentration. In the electrospinning process, solution concentration is the main factor that causes the charged polymer solution to stretch and bend in expanding loops to form a steady fibre formation [46,52]. According to Li Zhenyu and Wang Ce, [53] at a very low solution concentration, the charged polymer solution does not have strong polymer entanglements for fibre formation. Thus, this will cause instabilities during the electrospinning process and create an electrospraying phenomenon instead of electrospinning [54].

Furthermore, when electrospraying occurs, the surface tension of the polymer stream causes it to fragment into smaller droplets, as described in the Plateau–Rayleigh instability theory [55]. In contrast, when the solution concentration increases, the viscosity of the solution will increase; thus, the amount of polymer chains entanglement also increases [41,53,56]. Strong chain entanglements will overcome the surface tension and prevent the polymer stream from breaking up, producing smooth fibre formation (Figure. 3, left). However, at higher concentrations, the polymer solution will dry faster before it reaches the ground collector, hence resulting in the production of non-continuous fibre, larger diameter, and beaded structure, as shown in Figure 3 (right) [53,57]. In most electrospinning studies, beaded formation is known as defective nanofibre because beads will greatly reduce the surface-area-to-volume ratio of the nanofibres [58].

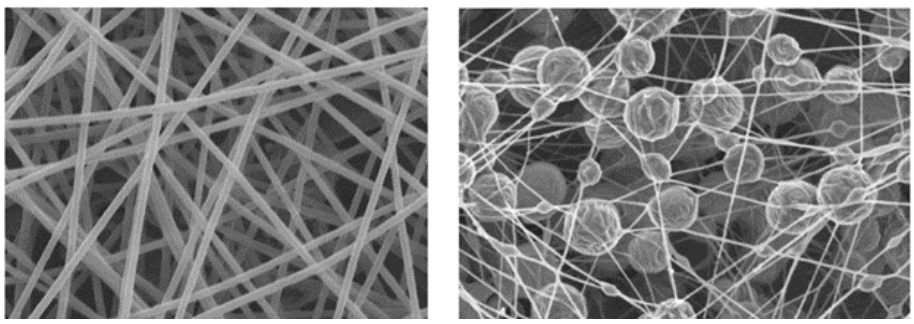

Figure 3. Formation of smooth (left) and beaded electrospun nanofibres (right) [58].

3.2 Applied Voltage

In the electrospinning system, the applied voltage is one of the most critical parameters to maintain the formation of polymer jets in a stable state and ensure the production of beadless fibres [46]. Fibres formation only occurs when the applied voltage (V) is higher than a threshold voltage (also called critical voltage, V_c) [17]. When the applied voltage (V) exceeds the minimum threshold voltage (V_c), the solution droplet will transform into a Taylor cone formation and begin to eject the polymer solution onto the grounded collector, as illustrated in Figure 4 [59]. Besides, at a low applied voltage, the electrostatic repulsive forces are not sufficient to overcome the surface tension of the polymeric solution, which results in no fibres formation [60].

On the other hand, increasing the applied voltage will create a balanced electric field and form steady polymer jets throughout the process [61–63]. For instance, a study by Bakar *et al.*, [64] stated that increasing the applied voltage will produce a stable repulsive force and stretch the fibres widely, thus resulting in a large fibre diameter with uniform fibre distributions. In contrast, contradictory findings had also been reported, where it was claimed that an increasing applied voltage would produce smaller fibre diameter [65]. The difference between these findings may be caused by the way other parameters were implemented. Apart from that, when the voltage applied is beyond the optimum range (value of the applied voltage at which beadless fibres are formed), the motion of the polymer jet will become unstable and produce non-uniform fibres with the presence of beaded structures [66]. Thus, optimising the applied voltage is critical in order to achieve balanced electric fields.

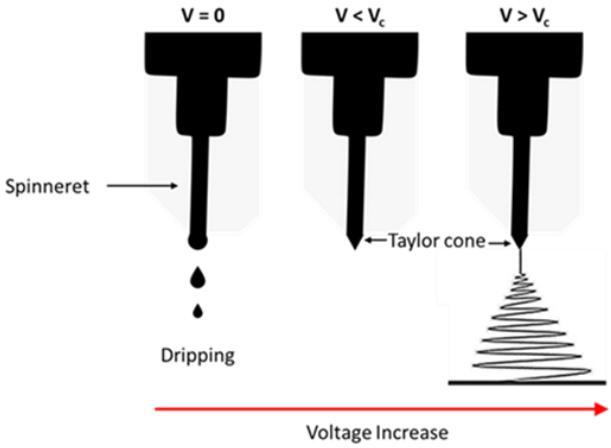

Figure 4. Schematic illustration of the Taylor cone formation at different voltages (critical voltage, V_c)

3.3 Electrospinning Distance

Electrospinning distance is defined as the distance between the tip of the spinneret to the grounded collector. Numerous studies have proven that the electrospinning distance has a significant effect on the production of electrospun nanofibers [67–69]. For instance, Nurfaizey and Munajat, [70] stated that if the electrospinning distance is too short, the area of deposition of fibres decreases. Thus, the polymer solution has insufficient time to evaporate before reaching the grounded collector (Figure 5). This situation causes the deposition of wet fibres, tendency to produce beaded fibres, or abnormally thick fibres [71]. On the contrary, as the distance increases, the duration of the electrospinning process increases, resulting in the formation of smooth and uniform electrospun nanofibres [72]. However, at a greater electrospinning distance, the electric field strength decreases, causing the system to require a higher voltage to maintain the process [71]. Otherwise, as the momentum of flying fibres decreases, the fibres would wander aimlessly, resulting in significantly less fibre formation on the collector electrode [73,74]. Therefore, when conducting the electrospinning process, the optimal electrospinning distance should be carefully

selected based on appropriate ranges. The most common electrospinning distance used in the literature is between 10 to 20 cm, also depending on other processing parameters [68,70–72].

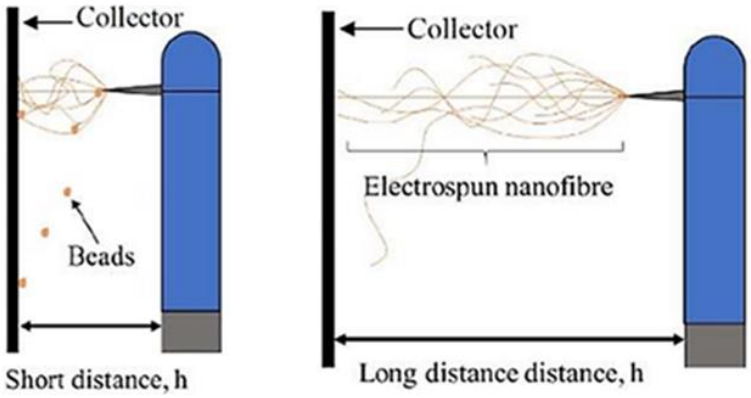

Figure 5. Schematic illustration of fibre production at different electrospinning distances, *h* [70]

3.4 Feed Rate

The formation of a stable polymer jet plays an indispensable and crucial role in fibre formation, which can be achieved by determining the optimum feed rate of the polymer solution [74–76]. As an example, excessive feed rate causes the motion of charged polymer jet to become unstable, resulting in the electrospray phenomenon, dripping of polymer droplets and producing large fibre diameter with abnormal structures [74]. In some cases, the capillary tips tend to detach from the spinneret because of massive electrostatic repulsive forces [77]. In addition, the excessive feed rate solution would cause the motion of charged polymer jet to be concentrated at a single point, resulting in the formation of clump fibres and bead structures [64,74]. Besides, the issue is exacerbated in a vertical electrospinning configuration (polymer jet moves downward), where the feed amount of polymer solution also increases due to gravitational force [78]. Hence, this will increase the tendency of beaded formation and non-uniform fibre distribution. Consequently, most of the electrospinning process currently has been done vertically, where the polymer solution is ejected steadily and has sufficient time to evaporate before reaching the grounded collector [79].

3.5 Ambient Temperature

Environmental factors are also important in the electrospinning process as it has been reported that relative humidity (RH) and working temperature also affect fibre diameter and morphological structure [80–82]. For instance, if the RH exceeds the optimum value, water molecules may permeate the fibres, preventing the fibre from completely drying out during the electrospinning process. Thus, producing a porous and wrinkled fibre texture, as shown in Figure 6 (right) [83,84]. In contrast, at an optimum RH typically in the range of 40 to 60%, smooth fibres texture and uniform orientation was observed [83–85]. Yang *et al.*, [82] stated that the working temperature also had an effect on the formation of nanofibres membranes. The authors stated that the diameter of the fibre decreased significantly from 500 nm to 200 nm as the working temperature increased from 20 to 80 °C. In fact, as the temperature increases, the solvent evaporates much faster, resulting in solid nanofibers with smaller fibre diameters and smoother surfaces. On the other hand, a lower working temperature would slower the evaporation process, producing wrinkles and rougher-surfaced fibres [81,82,86]. Hence, an in-depth understanding of electrospinning process parameters is required in order to produce uniform and smooth fibres formation, which has a significant impact on the performance of MD membranes. To this purpose, numerous researchers have investigated the effect of various processing factors, including providing the commonly used range of values for each parameter as given in Table 1.

Table 1. Summary of the Effect of Processing Parameters On the Morphology of the Electrospun Fibres

Process Parameter	Effects	Range Used In Literature
Solution concentration	Too high: The charged polymer solution dries faster, producing non-continuous fibre, large fibre diameter and beaded structures [57] Too low: Causing instabilities motion and create electrospraying phenomenon due to weak polymer chain entanglements [53]	6 to 12 wt% [46,53,54]
Applied voltage	Too high: Produced fibres with non-uniform diameters and with the presence of beaded structures [66] Too low: No fibre formation due to insufficient electrostatic repulsive forces [60]	10 to 20 kV [59,60,66]
Electrospinning distance	Too long: Inconsistent fibre deposition due to weak electric field strength [71] Too short: Produced wet fibres due to the solvent does not entirely evaporate [70].	10 to 20 cm [68,70–72].
Feed rate	Too high: Produced large fibre diameter, increased fibre wetness and beaded structures [74] Too low: Produced small fibre diameter and less fibre formation [74]	0.5 to 1.5 ml/h [61,87–90]
Ambient temperature	<u>Working temperature</u> Too high: Produced poor fibre texture and large fibre diameter with beaded structures [91] Too low: Produced wet fibre, wrinkles and rougher-surfaces fibres [55] <u>Humidity</u> Too high: Produced porous and wrinkled fibre textures due to absorption of water molecules [84] Too low: Produced non-continuous fibre and brittle structures [85]	25°C (room temp.) [34,88] 40 - 60 % [83,84]

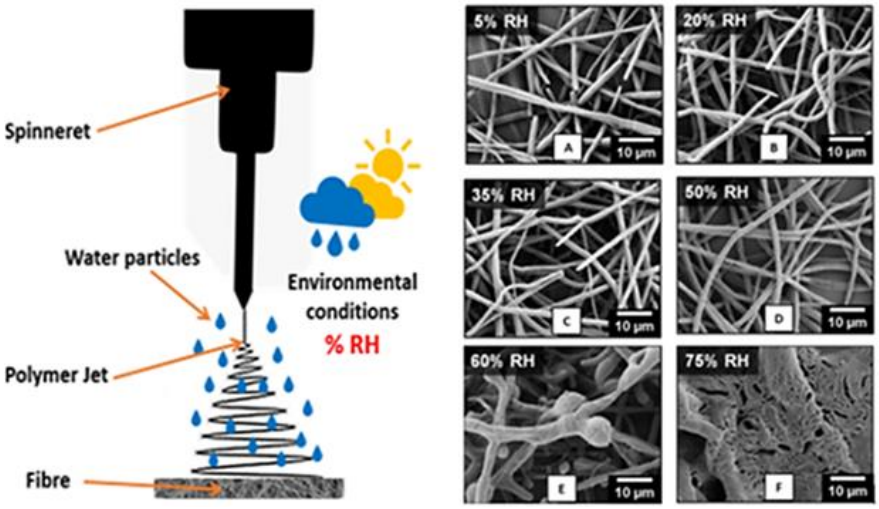

Figure 6. Schematic drawing of the electrospinning process exposed to ambient temperature (left) and SEM micrographs of electrospun nanofibres at different relative humidity (RH) [85] (right).

4. CHARACTERISTICS OF POLYACRYLONITRILE IN DEVELOPMENT OF MEMBRANE MODULE FOR THE MEMBRANE DISTILLATION PROCESS

The developed membrane module ought to fulfil specific requirements before it can be applied for the desalination process. For instance, the membrane should be made from hydrophobic materials with high porosity structures [92]. Moreover, the size of the membranes pore should be small as possible in order to achieve high permeate flux and to prevent membrane wetting [93–95]. Aside from that, membrane thickness is also an important factor because an increase in membrane thickness will increase the resistance of vapour transmissions, resulting in a decrease in vapour flux [96,97]. On the other hand, the membrane material should have a low thermal conductivity, excellent thermal stability and chemical resistance, and high mechanical properties to ensure that MD membranes have a long lifespan with a stable MD performance [98]. Hence, PAN electrospun fibres have a huge potential in developing high-performance membrane modules for MD system due to their superior characteristics.

4.1 Fibre Diameter and Pore Size

Fibre diameter and pore size can be characterised either using a transmission electron microscope (TEM), field emission SEM (FE-SEM), or scanning electron microscope (SEM) [99]. According to the literature, the average fibre diameter of PAN electrospun nanofibers is typically between 100 and 800 nm, depending on the processing parameters and experimental setup [62,100–103]. As an example, Celep and Dincer, [104] use the Taguchi method to optimise the electrospinning process parameters in producing PAN electrospun nanofibres. Taguchi's L_{16} orthogonal design method (4 parameters, 4 levels) was selected as the process parameters consisted of four main parameters: applied voltage, electrospinning distance, polymer feed rate, and polymer concentration. The signal-to-noise (S/N) ratio was used to describe which set of parameters provided better fibre morphology, which was determined by observing the fibre diameter using the approach "the smaller, the better". Based on both experimental and analysis methods, the optimal parameters observed were 8 wt% of solution concentration, 10 kV of applied voltage, 2.5 ml/h of polymer feed rate, and 12 cm of electrospinning distance. The obtained PAN electrospun nanofibres produced under optimal conditions showed no beads formation and had a fibre diameter of 163.6 nm.

Fibre diameter in the nanoscale range is favourable because a smaller fibre diameter with smooth surfaces will enhance the MD performance by forming a dense porous structure. Contrarily, a larger fibre diameter results in a more open structure, which leads to a higher particle passing through the membrane pores, resulting in decreased filtration efficiency [105]. Furthermore, the membrane with a proper pore size and a highly porous structure could increase the vapour flux due to increased evaporation surface area [106]. Typically, the pore size of the hydrophobic membrane used in the MD process was less than 1 μm. Otherwise, the membrane's surface energy and hydrophobicity would decrease, resulting in membrane wetting and lowering the salt rejection efficiency [107]. According to Roche and Yalcinkaya, [108] the average pore size for PAN electrospun nanofibres is between 0.4 - 0.7 μm, where this range of values is highly recommended for the MD process. Besides, PAN electrospun nanofibres have a narrow pore size distribution and a porosity of approximately 80 – 90 %, making them highly effective at removing submicrometre and micrometre particles from air and water [22,100,108].

4.2 Surface Hydrophobicity

Surface hydrophobicity, also known as surface wettability, refers to the capability of a surface to repel water, which can be determined by measuring the water contact angle (WCA) between a water droplet interface and a solid surface [109]. Surface hydrophobicity is classified into three categories: superhydrophobic ($\theta \geq 150°$), hydrophobic ($90° \leq \theta < 150°$), and hydrophilic ($0° \leq \theta < 90°$). In the MD system, only water vapour or gas molecules can be passed through the membrane

pores, which indicate that surface wettability plays an important role in determining membrane performance. Moreover, throughout the evaporation process, vapour will pass through membrane pores from the hot feed-side into the cold permeate-side with a certain amount of pressure. This pressure is known as liquid entry pressure (LEP). According to Shahabadi *et al.*, [110] in order to achieve a long-lasting MD process, the value of the membrane LEP should be as high as possible in order to avoid membrane wetting. Thus, the membrane module with a superhydrophobic surface is highly recommended since it can delay the ageing of the membrane surface, enhance the antifouling properties, and increase the permeate flux [111,112]. Although PAN nanofibres are classified as hydrophobic membranes (WCA is typically between 100° and 130°) [113–116], the surface hydrophobicity can be increased with the addition of fluorinated materials and nanoparticles compounds to reduce its surface energy and increase surface roughness [117,118].

Recently, fluorinated-based materials are often used in the development of membrane filters where the combination of these substances with hydrophobic polymer will result in a high contact angle [119]. Fluorinated compounds or fluorinated polymers are known as materials with extremely low surface energy because the presence of CF_3 groups in the polymer structures will weaken the intermolecular bonds [120]. For example, Almasian *et al.*, [121] synthesised triethylenetetramine (TETA) and 1H,1H,2H,2H-Perfluorodecylacrylate (PFDA) at different solution concentrations to create a fluoroamine compound. The fabricated PAN electrospun nanofibres were immersed in the fluoroamine compound and then dried in an oven at a temperature of 80°C for 24 hours. Based on TEM analyses (Figure 7), the fluorinated PAN nanofibre formed a dense skin layer. The WCA observed for fluorinated PAN nanofibre at optimum conditions was 159.2° with a skin layer thickness of 13 nm. This finding shows that using fluorinated treatments can significantly increase WCA due to the presence of a skin layer, which increases the surface roughness of the nanofibre membranes.

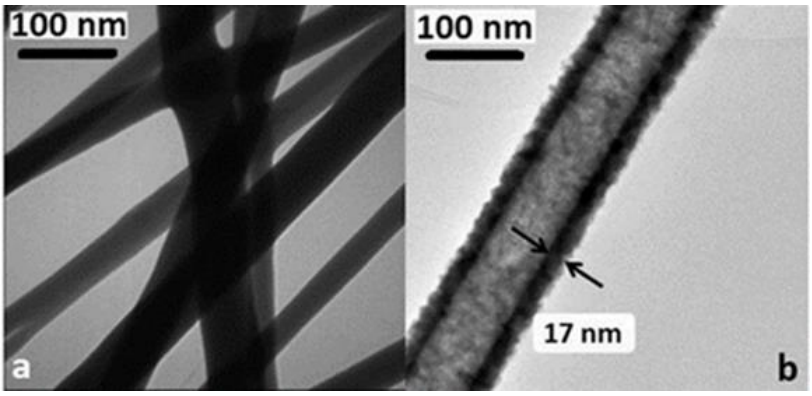

Figure 7. TEM micrograph of PAN nanofibres: a) untreated b) fluorinated PAN [121].

Furthermore, another common method to fabricate superhydrophobic nanofibres is using nanoparticles compounds such as silica (SiO_2), titanium (TiO_2), and zinc (ZnO) [6]. For instance, Rostami *et al.*, [122] fabricated superhydrophobic PAN nanofibrous filters by preparing three different coating solutions of nanoparticles (ZnO, TiO_2, and boehmite nanoparticles). The prepared PAN nanofibres were immersed in the respective nanoparticle solutions via dip-coating technique for 60 seconds and then dried at 23°C for 5 min. The coating process was repeated two times and kept at 50°C for two days to ensure the solvent completely dried. As a result, the WCA of the treated PAN nanofibres increased from 116° to 152°, 168°, and 141° for boehmite, ZnO, and TiO_2 nanoparticles, respectively, as shown in Figure 8. The presence of nanoparticles in nanofibres surface reduces the size of membrane pores and increases surface roughness, preventing water droplets from penetrating the membrane [123].

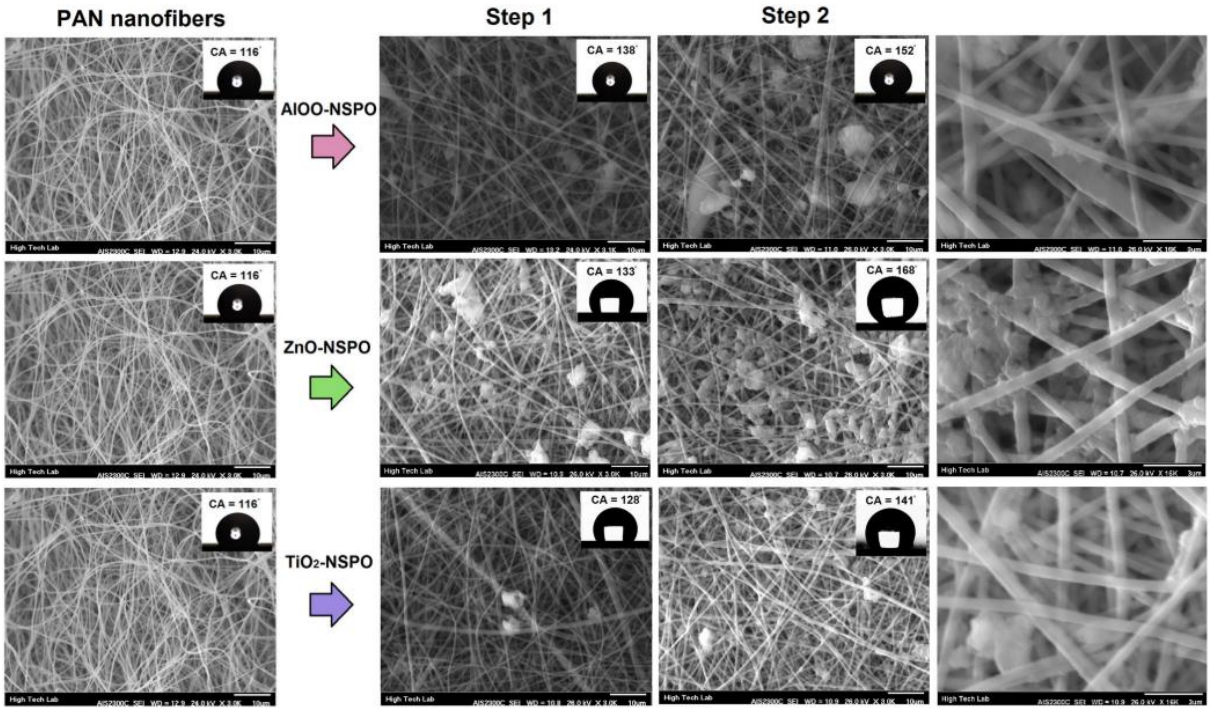

Figure 8. SEM images of PAN electrospun nanofibres coated with modified boehmite (Aloo-NSPO), zinc (ZnO-NSPO), and titanium nanoparticles (TiO_2-NSPO). The WCA for each condition is shown at the top right corner [122].

On the other hand, the WCA of PAN nanofibres can also be increased by performing stabilisation and carbonisation processes, which will increase the surface roughness due to the presence of the bumpy surface [124]. Alarifi *et al.*, [125] fabricated PAN carbon fibres by stabilising them in an oxygen atmosphere at 270 ˚C for 60 min, followed by carbonisation. The carbonisation process was performed under different temperatures (750, 850, and 950˚C) in an inert atmosphere for 60 min. The results showed that the WCA of PAN carbon fibres increased from 155° to 160° as the carbonisation temperature increased. During the stabilisation and carbonisation process, the PAN fibres experienced thermal expansion and structural changes, resulting in the forming of cross-links structures that significantly affected the WCA [126]. Hence, this approach highlighted that it is necessary to perform stabilisation processes in developing membrane modules to enhance the characteristics and performance of PAN-based membranes.

4.3 Thermal Behaviour

Solvent resistance and thermal stability are the critical factors that significantly affect the performance of the MD membrane during the filtration process. In order to design a membrane module that can survive high temperatures while maintaining an intact pore structure as in its original condition, the developed membrane should have good thermal stability, which can prevent any deformation [127]. Thermogravimetric analysis (TGA) and differential scanning calorimetry (DSC) are the most common tools in determining the thermal behaviour of PAN membranes [128]. PAN membrane consists of a chain of carbon connected to one another, which makes them physically stronger than other polymeric precursors [129,130]. Moreover, PAN membranes have excellent thermal stability without obvious thermal distortion [131]. As an example, Alarifi *et al.,* [132] performed TGA analysis and found out that the virgin PAN nanofibres had no weight loss during the first stage of TGA analysis (302°C). At the second and third stages (302 - 571°C), the weight of PAN nanofibre decreased by 18%, indicating that there was a change in molecular structure. In the final stage (571 - 732°C), the observed weight loss was 80%, which means that the polymer chain of the PAN nanofibres was completely evaporated when the

temperature was above 730°C. This finding demonstrated that pure PAN electrospun fibres were capable of withstanding high temperatures without any deformation.

The glass transition temperature (T_g) and melting temperature (T_m) of PAN are commonly in the range of 110 - 130°C and 335 - 360°C, respectively [133,134]. However, to achieve the desired fibre membrane, the membrane should undergo a stabilisation process that will enhance the molecular structure of the fibres. In fact, when PAN membrane experiences a thermal stabilisation process at a temperature range of 200-300°C (in the air atmosphere), three major stabilisation reactions will occur simultaneously, which are cyclisation of the nitrile groups, dehydrogenation, and oxidation [135,136]. In particular, cyclisation is the main reaction which forms a cross-linked ladder structure that converts $C \equiv N$ into $C = N$ [136,137]. Consequently, the chemical stability and mechanical properties of the ladder structure increase drastically due to the ring formation that strengthens the intermolecular bonds, as demonstrated in Figure 9 [138]. Meanwhile, the dehydrogenation reaction creates conjugated structures on the main chain of PAN polymer that changes $C - N$ into $C = N$ [139]. Oxidation reactions produce infusible and stronger ladder polymer structures that can withstand higher temperatures during the carbonisation process [140,141]. Additionally, after the stabilisation process, the colour of PAN fibres change from white/pale yellow into a darker colour (brown), which indicates the transformation of thermoplastic to a thermoset [102,139,140,142].

Apart from that, the advantage of the thermal stabilisation process is that it will prevent fibre shrinkage and maintain the molecular structure [143]. However, if the stabilisation process occurs rapidly, it will lead to excessive fibre shrinkage, extreme mass loss, and even melting. In contrast, a slower stabilisation process will partially stabilise the fibre, which can cause defects in the formation of a cross-linked structure [144]. Currently, the stabilisation of PAN polymer has been a topic of research for many years due to its advantages in producing high-quality membrane modules [145]. For instance, Wu *et al.,* [145] discovered huge differences between PAN nanofibres that underwent the stabilisation process and those that did not. Results demonstrated that normal PAN nanofibres began to degrade rapidly at 280°C, whereas stabilised PAN nanofibres began to degrade at temperatures ranging from 310°C to 345°C (Figure 10). However, when the temperature was raised to 600°C, the residual weight for normal PAN nanofibres observed was 36%, while the residual weight for stabilised PAN nanofibres was 73%. Therefore, by undergoing the stabilisation process, the amount of carbon yield in the PAN nanofibres increases drastically, which can contribute to the production of high-performance membranes that can be applied for various industrial applications [129,137,146].

Furthermore, since MD is a non-isothermal process, the active layer of the membrane should be made of a material with low thermal conductivity to prevent heat loss during the desalination process. For this purpose, the thermal conductivity for the MD membrane must be below 0.2 W/mK to ensure a stable vapour flux and thermal efficiency [98]. Tao *et al.,* [147] managed to develop a super-low thermal conductivity fibrous nanocomposite by using PAN as precursor material and hollow silica sphere as the filler. The authors found that as the content of hollow silica spheres increased, the thermal conductivity of PAN membrane decreased from 0.054 W/mK to 0.016 W/mK. Interestingly, by embedding hollow silica spheres or nanoparticles into the nanofibres membrane, the micropore size can be reduced, thereby minimising the amount of heat transferred through the membrane pore [148]. Thus, based on previous research, PAN electrospun nanofibre membrane demonstrated excellent thermal insulating properties via a combination of micrometre and nanometre porous structure, making it an ideal candidate for the development of membrane modules for MD system [147,149].

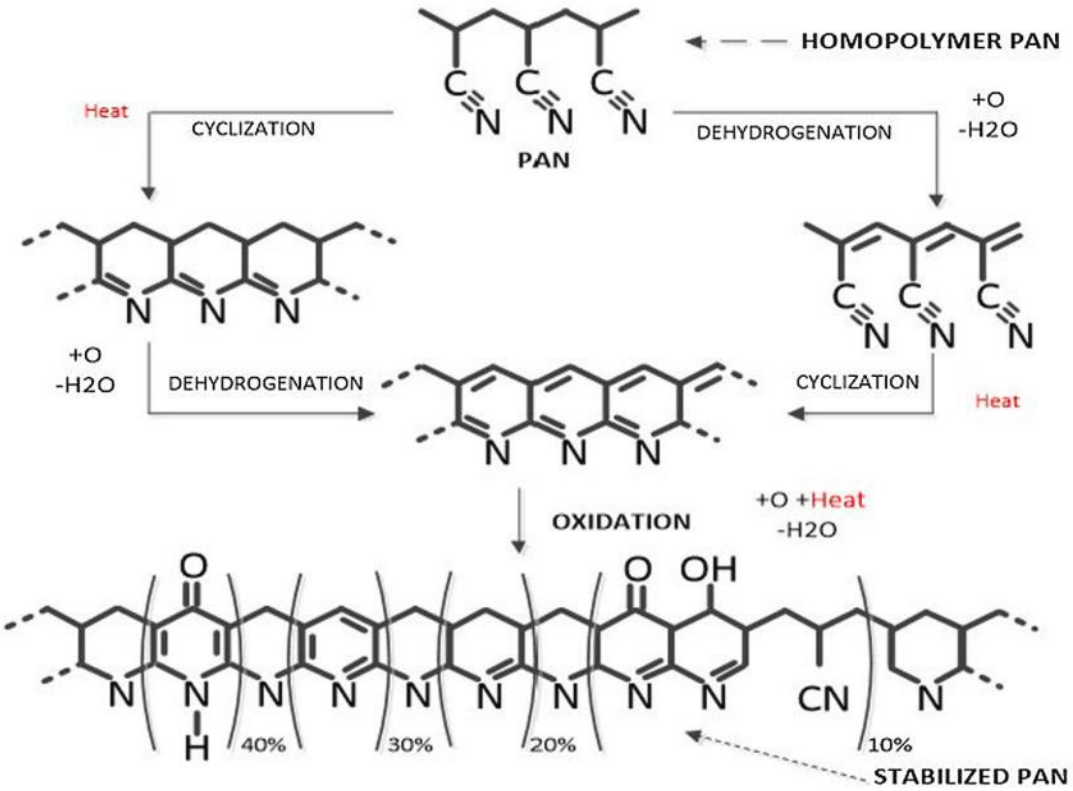

Figure 9. Reactions involved in stabilisation of PAN [129].

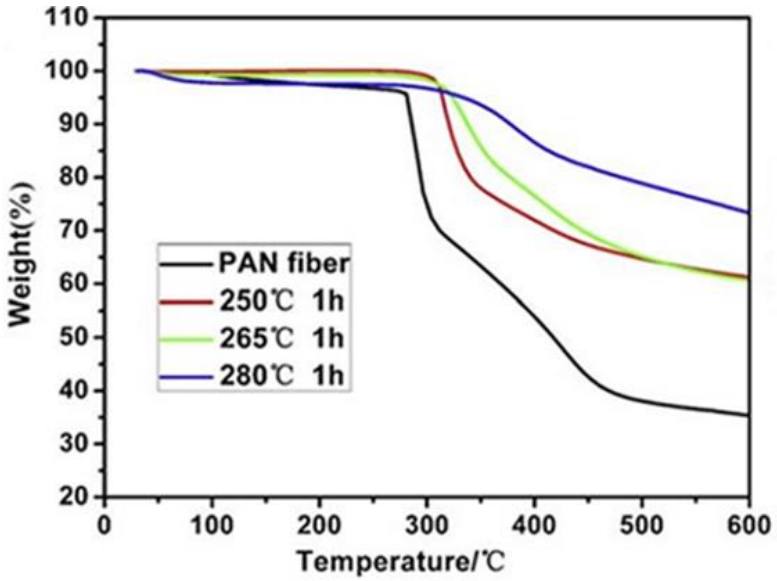

Figure 10. TGA curves of PAN nanofibres after being stabilised at different temperatures [145].

4.4 Tensile Behaviour

A high strength membrane with optimum thickness is one of the important criteria that could affect the membrane lifespan and vapour flux during the operation [98,150]. The mechanical properties of PAN electrospun nanofibres are typically affected by several factors such as fibre alignment, fibre diameter, fibre thickness, solution concentration, pre-oxidation temperature and the addition of other reinforcements materials [151–155]. For example, Liu *et al.,* [154] prepared

PAN/DMF solutions with varying concentrations (8 to 14 wt%), which were then electrospun at a fixed tip-to-collector distance, applied voltage, and solution feed rate. The authors revealed that the tensile strength of PAN nanofibres increased from 1.6 MPa to 6.88 MPa as the concentration increased. A similar finding was also reported by Khan et a. [61], who mentioned that the tensile strength increased from 3.56 to 15.86 MPa as the concentration increased from 6 to 12 wt%. The increase in tensile strength is caused by the fibre diameter and homogeneous factors, which directly influence the tensile properties and modulus of electrospun nanofibres [156].

Karim *et al.*, [150] found that adding other reinforcements materials such as carbon nanotubes (CNT) into PAN nanofibres would increase the mechanical properties. The authors also stated that the PAN/CNT composite nanofibre had better mechanical properties at a low concentration of CNTs (0.1 wt%). On the contrary, at high concentration, the decrease of tensile strength and Young's modulus were observed. The tensile strength of pure PAN and PAN/CNT composite nanofibres were 55.2 MPa and 122 MPa, respectively. This result showed that the increase of mechanical properties could be attributed to the aspect ratio of the CNT, which increases the strength and stiffness of the PAN/CNT structural bonding [157]. Besides, PAN homopolymer is made up of a triple bond (C_3H_3N) that contains nitrogen molecules. The addition of CNT filler will increase the number of triple bonds in composite nanofibres, which strengthens the interactions between PAN/CNT molecular bonds [23,158]. However, if there are excessive amounts of CNT filler in composite nanofibres, the tensile strength will decrease drastically due to the high number of triple bonds in the polymer chains [150,158]. Due to their excellent mechanical properties, PAN/CNT nanofibres can be applied in the development of membrane filters to remove organic dyes, metal ions, and bacteria from aqueous solutions effectively [159].

On the other hand, Duan *et al.*, [160] fabricated PAN nanofibres membranes via the electrospinning technique, which were then stabilised at different temperatures in an air atmosphere for 1 hour. The authors discovered that the tensile strength increased from 5 MPa to 30 MPa as the annealing temperature was raised to 260°C. However, when the annealing temperature exceeded 260°C, the tensile strength began to decrease. This is because the weight of PAN nanofibres began to degrade, which indirectly changed the molecular structure of the polymer chains [145]. In another study, Lee *et al.,* [161] prepared PAN fibres that were stabilised at a constant temperature of 250°C with different holding times (5 to 180 min). The results showed that there were no significant changes in the first 30 min, whereas a further increase in the holding time would lead to a monotonic decrease in the tensile strength. Nevertheless, when the PAN fibres were heated for a long period of time and reached the melting temperature (T_m), the ladder structure was disrupted due to the crystalline and orientation structure [133,162]. Thus, the tensile strength of the stabilised PAN fibres was lower compared to pure PAN fibres.

Furthermore, Arif *et al.*, [163] mentioned that membrane thickness also influenced the tensile strength of PAN electrospun fibres. As membrane thickness increased, the tensile strength also increased. Based on previous research, the average thickness of PAN fibres ranged between 3 and 30 μm, which was within the range of the optimum thickness [163,164]. The optimum membrane thickness for the MD process was reported to be between 10 to 60 μm [165,166]. Besides, in the development of membrane modules, the membrane thickness plays an important role because as the membrane thickness increases, the diffusion distance between the hot feed-side and cold permeate-side increases, resulting in lower vapour flux [98]. Moreover, it was suggested that the hydrophobic membrane should be as thin as possible and possess high mechanical strength. Therefore, PAN electrospun nanofibres are thought to be a promising choice as a foundation material or supporting layer in the development of membrane modules due to the above-mentioned characteristics. The characteristics of PAN electrospun fibres and benchmarks for optimum MD membranes are summarised in Table 2.

Table 2 Characteristics of PAN Electrospun Fibres and MD Requirements

Characteristics	MD requirement	PAN Electrospun Fibres
Pore size	10 nm - 1 μm [106]	0.3 - 0.8 μm [88,108]
Pore size distribution	Narrow [98]	Narrow [100]
Porosity	More than 80 % [92,98]	80 - 90 % [22,100]
Contact angle	More than 90° [92]	110 - 130° [113,115,116]
Thermal conductivity	Less than 0.2 W/mK [98]	0.02 - 0.04 W/mK [147,149]
Membrane thickness	10 - 60 μm [98]	3 - 30 μm [163,164]

5. CURRENT APPLICATION OF POLYACRYLONITRILE ELECTROSPUN FIBRES IN THE DEVELOPMENT OF MEMBRANE MODULE

MD is theoretically known as one of the best membrane systems due to its higher salt rejection efficiency, lower energy consumption, and capability to operate at low temperatures [8,9]. MD has four main configurations, which are air gap membrane distillation (AGMD), sweeping gas membrane distillation (SGMD), vacuum membrane distillation (VMD), and direct contact membrane distillation (DCMD) [167,168]. Although MD typically has an almost 100 % salt rejection efficiency, full industrial implementation of MD is still a challenge due to the uncertainty of its process efficiency and operational costs [93,169,170]. The other reasons are the low vapour flux and membrane wetting, which always occur when the membrane is utilised for a longer time period [171]. Hence, in order to overcome these issues, the developed membranes must meet all of the MD requirements as listed in Table 2.

Membrane modules are classified into four types which are hollow fibre, plate and frame, spiral wound and tubular membrane [106]. In particular, hollow fibre membrane has a large membrane area to modulate volume ratios, and this makes it more favourable in the fabrication of membrane modules [172]. Currently, researchers have developed a variety of membrane designs using PAN electrospun fibres as a precursor material. For example, triple-layered structure, dual-layered structure, core-shell fibrous structure, and surface coating and modification. In general, by selecting the proper approach and optimum process conditions, the properties of the membrane module can be modified to a higher level.

5.1 Dual-Layered Membrane

Cai *et al.*, [173] create dual-layered nanofibrous membranes by using polyvinylpyrrolidone (PVP) as a thin skin layer and PAN as a thick supporting layer. The skin layer was electrospun onto the surface of a 50 μm thick supporting layer. The composite fibrous membranes demonstrated a stable vapour flux of 19.2 kg m^{-2} h^{-1} and a salt rejection efficiency of 99.98 %. Combination of skin layers with varying pore sizes and porosity, resulting in a larger contact angle (greater than 150°) due to rougher surface and low surface energy. Remarkably, this approach can be used to modify a porous membrane with a large pore size so that it can be used in MD systems without compromising its performance.

Woo *et al.*, [174] used a similar method to create a dual-layer nanofibre nonwoven membrane for the AGMD configuration. The top layer was fabricated using a hydrophobic polyvinylidene fluoride-co-hexafluoropropylene (PH) membrane. Meanwhile, the hydrophilic supporting layer was made with different substrates (Figure 11). Each substrate was electrospun directly to the drum collector, followed by the electrospinning of PH nanofibres on the surface of the supporting layer membrane. The composite membranes were dried at 60° C for 48 hours and then underwent heat-press treatment inside an oven with a temperature of 170° C for 90 minutes.

Among these composite membranes, the combination of Nylon 6 and PH nanofibre membranes with a thickness of 92 μm provided better performance in terms of vapour flux and salt rejection, with values of 15.5 kg m^{-2} h^{-1} and 99%, respectively. Contrarily, Tijing *et al.*, [175] came up with different conclusions, where the authors observed that PH/PAN nanofibres membrane with 80 μm thickness possessed the highest vapour flux of 30 kg m^{-2} h^{-1} and a salt rejection efficiency of more than 98.5 %. The discrepancy between these findings is thought to be due to the different membrane thickness that significantly affects the vapour flux.

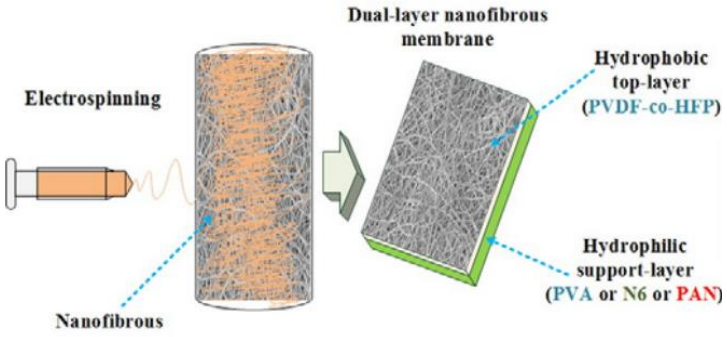

Figure 11. Schematic drawing of the preparation of the double-layered membrane [174].

5.2 Triple-Layered Membrane

Efome *et al.*, [176] take a different approach by creating triple-layered nanofibrous membranes using PAN as one of the main materials. The top layer of the membranes was made from polyvinylidene fluoride (PVDF) mixed with hydrophobic silica nanoparticles. Electrospun polyvinylidene fluoride (PVDF) was used as the top layer, along with hydrophobic silica nanoparticles. The middle layer was composed of PAN nanofibers and metal-organic frameworks, while the bottom layer was composed of PVDF and hydrophilic silica nanoparticles. These materials were electrospun layer by layer, as illustrated in Figure 12. The concept behind this triple-layered membrane is that the top hydrophobic layer prevents feed water from entering, followed by a middle layer with a large pore size to minimise resistance during vapour transmission, and the hydrophilic layer at the bottom is responsible for transmembrane vapour flux to the permeate-cold side. However, the disadvantage of this method is that the obtained vapour flux was only 4.4 kg m^{-2} h^{-1}, which was caused by the large membrane thickness (>600 m). Thus, for future research, the membrane should undergo cold-pressed treatment in order to achieve the desired thickness.

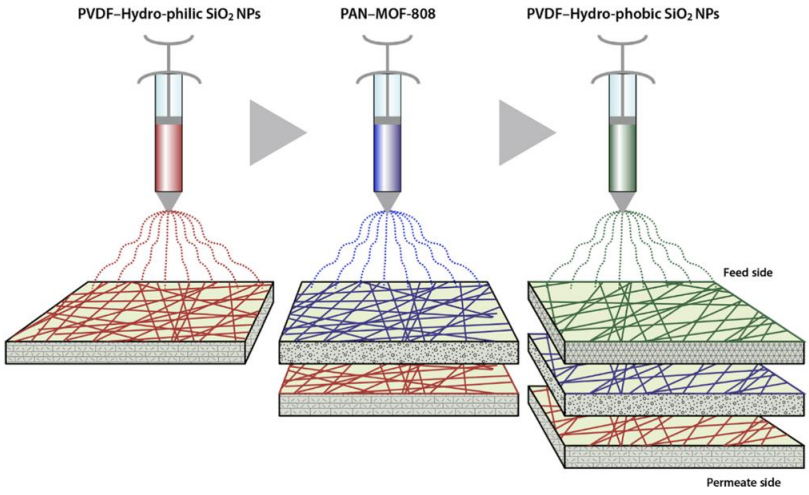

Figure 12. Schematic drawing of the preparation of the triple-layered membrane [176].

5.3 Core-Shell Membrane

Li *et al.*, [177] developed a core-shell polyacrylonitrile-polystyrene (PAN-PS) nanofibre membrane using the coaxial electrospinning technique. Coaxial electrospinning is a technique that ejects two polymer solutions simultaneously through a modified spinneret composed of two coaxial capillaries with different orifice sizes (Figure 13). The obtained core-shell electrospun nanofibres were placed in a vacuum oven at 60°C for 12 hours before being cold-pressed at room temperature to achieve the desired thickness (100 µm). The average fibre diameter and WCA for PAN-PS core-shell nanofibres membrane observed was 750 nm and 151.3°, respectively. Apart from that, the developed membrane provides excellent results, with a vapour flux and salt rejection efficiency of 60.1 kg m^{-2} h^{-1} and 99.99%, respectively. This could be due to the eccentric-axial electrospinning technique, which creates a unique groove structure that possesses a high membrane void volume ratio and good thermal stability. In addition, this approach also demonstrated that the void volume fraction was a significant factor in the enhancement of mass transport (vapour flux) in the MD process. As the void volume fraction increased, the water vapour permeates flux also increased.

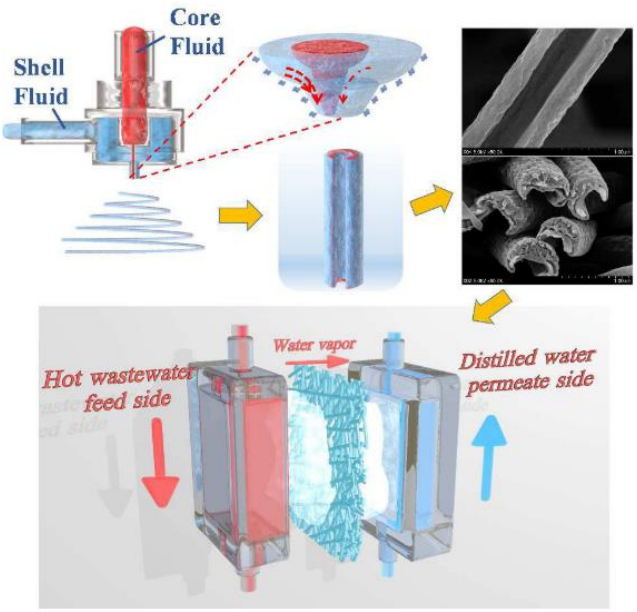

Figure 13. Schematic diagram illustrating the eccentric-axial electrospinning technique for the fabrication procedure of grooved core-shell nanofibrous membranes [177].

5.4 Surface Coating and Modification

In another study, Tang *et al.*, [178] developed asymmetric wettability composite membranes using PAN nanofibres and polytetrafluoroethylene (PTFE) flat sheet membranes. The fabrication process began with electrospinning of PAN fibres on a hydrophobic PTFE membrane surface, followed by a hydrolysis treatment with ethylenediamine (EDA) and sodium hydroxide (NaOH). The main focus of this approach is to create a membrane with anti-oil-fouling characteristics for desalinating high salinity and oily wastewaters. The composite membranes were tested using the DCMD process, which contained saline water and crude oil at the feed side. The results were positive, where the modified composite membrane showed excellent results with 100% salt rejection efficiency and performed steady permeate flux with 15.2 kg m^{-2} h^{-1}. Besides, the composite membrane also demonstrated superoleophobicity characteristics, with an oil contact angle of more than 150°. Thus, this approach could be used as an anti-oil-fouling MD membrane for desalinating challenging saline and oily wastewater.

Furthermore, Qin *et al.*, [179] managed to create a high-performance composite membrane by combining PAN nanofibres, nanofibre cellulose (NC) solution, and a PVA-based film. PAN electrospun nanofibres were immersed in hydrochloric acid (HCL) for approximately two minutes, followed by surface coating with 0.5 wt % of NC solution using the casting knife technique. The PAN-NC nanofibres membrane was dried at room temperature (25°C) for 120 minutes before being placed in a vacuum oven at 60°C for 4 hours. Lastly, the treated PAN nanofibres were spray-coated with PVA solution and dried at 100°C for 15 minutes. The membrane thickness of PVA/NC-PAN observed was 3.78 μm with an average pore size of 150 nm. Figure 14 shows a schematic drawing of the PVA/PAN-NC nanofibres membrane. The fabricated composite nanofibre membranes exhibited extradentary pervaporation desalination properties, with a water flux of 238.7 kg m^{-2} h^{-1} and a salt rejection efficiency of 99.8%. To the best of the authors' knowledge, this method provides the highest vapour flux in desalination technologies when compared to other PAN-based membrane modules. Additionally, this method established that membrane thickness, pore size, and surface hydrophobicity play important roles in increasing vapour flux while maintaining salt rejection efficiency. Therefore, it is critical to consider the entire MD requirements when developing a new membrane module in order to achieve optimal MD performance. A summarised list of the various membrane preparation techniques used in the MD system is given in Table 3.

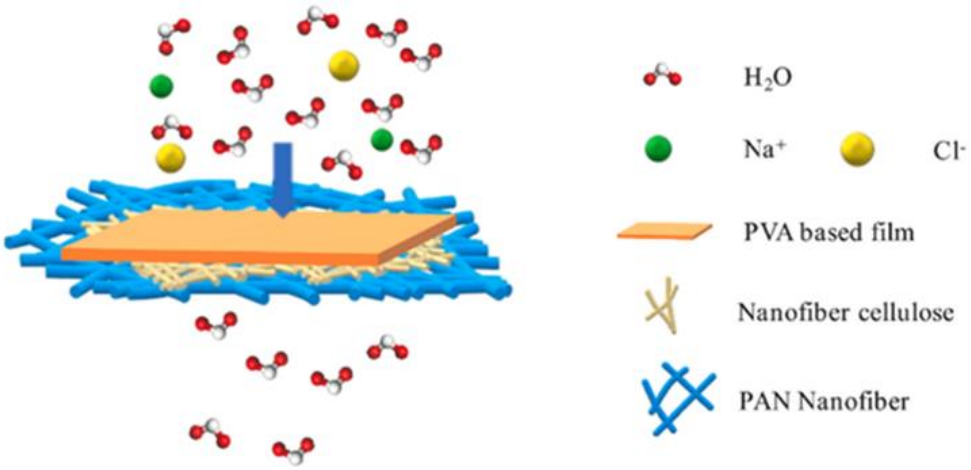

Figure 14. Schematic drawing of the desalination process using PVA/PAN-NC nanofibres membrane [179].

Table 3 A Summarised List of the Recent PAN-based Membrane Preparation Techniques

Membrane Design	Polymer	Membrane Preparation Technique	Vapor Flux (kg $m^{-2} h^{-1}$)	Salt Rejection Efficiency (%)	Ref.
Dual-layered structure	PAN, & PVDF-HFP	Electrospun layer by layer, PVDF-HFP (skin layer) & PAN (support layer)	30.0	99.90	[175]
	PAN & PVP	Electrospun layer by layer, PVP (skin layer) & PAN (support layer)	19.2 ± 1.2	99.98	[173]
	PAN & PTFE	Electrospun PAN onto the surface of PTFE flat sheet membrane, EDA & NaOH hydrolysis	15.2	100.	[178]
Triple-layered structure	PAN & PVDF	Electrospun layer by layer, PVDF-hydrophobic / hydrophilic SiO_2 nanoparticles (top & bottom layer) & PAN nanofibres (middle layer)	4.4	99.99	[176]
Core-shell structure	PAN & PS	Electrospinning, PAN (core solution) & PS (shell solution)	60.1	99.99	[177]
Surface coating & modification	PAN, PVA	Electrospinning, PAN nanofibres immersed in HCL, NC surface coating & spray coated with PVA solution	238.7	99.80	[179]
	PAN & PFDA	Surface fluorination treatment, PFDA vapour permeated into the surface of PAN electrospun fibres	11.0	99.99	[180]

6. CONCLUSION

Polyacrylonitrile (PAN) is considered a promising precursor material for the development of high-performance membrane modules due to its superior properties. PAN fibres produced via electrospinning exhibited remarkable properties such as a hydrophobic surface, nanoscale fibre diameter, porous structure, and high mechanical strength. However, in order to obtain the desired membrane properties, the main electrospinning parameters (solution concentration, applied voltage, electrospinning distance, solution feed rate, and ambient temperature) must be optimised until smooth fibres without bead structures are formed. It is suggested to adhere to the range of values specified in Table 1 for each electrospinning process parameter. Additionally, there are several criteria that need to be highlighted during the development of membrane modules, including pore size, pore size distribution, porosity, water contact angle, thermal conductivity and membrane thickness. These criteria significantly affect the performance of the MD process in terms of vapour flux and salt rejection efficiency. Apart from that, characteristics of PAN electrospun fibres meet all MD requirements and may be better compared to other hydrophobic materials (refer to Table 2). Hence, numerous research efforts have been made to develop PAN-based fibre membranes with a variety of fabrication methods, such as dual-layered structure, triple-layered structure, core-shell structure, and surface coating and modification. However, improvements in vapour flux and membrane wetting are still required to develop optimal membranes that produce positive outcomes with cost-effective implementation. In conclusion, this review provides some useful guidance for future research activities concerning the optimum electrospinning process parameters, the characteristics of PAN electrospun fibre, and its potential application in the development of membrane modules for MD systems.

ACKNOWLEDGEMENTS

The authors would like to thank the Ministry of Higher Education Malaysia and Universiti Teknikal Malaysia Melaka through the funding of Collaborative Research Grant PJP/2019/FKM-CARE/CRG/S01706. Special thanks to the members of Advanced Materials Characterization Laboratory (UTeM), Academia-Industry Collaboration Laboratory, the members of the Faculty of Mechanical Engineering, UTeM, and Advanced Membrane Technology Research Centre (AMTEC), UTM.

REFERENCES

[1] van Vliet, M. T. H., Jones, E. R., Flörke, M., Franssen, W. H. P., Hanasaki, N., Wada, Y., and Yearsley, J. R., Environ. Res. Lett. vol **16**, issue 2 (2021) .
[2] Kugarajah, V., Ojha, A. K., Ranjan, S., Dasgupta, N., Ganesapillai, M., Dharmalingam, S., Elmoll, A., Hosseini, S. A., Muthulakshmi, L., Vijayakumar, S., and Mishra, B. N., J. Environ. Chem. Eng. vol **9**, issue 2 (2021) p.105107.
[3] Zhang, D., Sial, M. S., Ahmad, N., Filipe, J. A., Thu, P. A., Zia-Ud-din, M., and Caleiro, A. B., Sustain. vol **13**, issue 1 (2021) pp.1–10.
[4] Pistocchi, A., Bleninger, T., Breyer, C., Caldera, U., Dorati, C., Ganora, D., Millán, M. M., Paton, C., Poullis, D., Herrero, F. S., Sapiano, M., Semiat, R., Sommariva, C., Yuece, S., and Zaragoza, G., Water Res. vol **182** (2020) .
[5] An, A. K., Guo, J., Jeong, S., Lee, E. J., Tabatabai, S. A. A., and Leiknes, T. O., Water Res. (2016) .
[6] Li, S., Huang, J., Chen, Z., Chen, G., and Lai, Y., J. Mater. Chem. A vol **5**, issue 1 (2017) pp.31–55.
[7] Roy, S., Humoud, M. S., Intrchom, W., and Mitra, S., ACS Sustain. Chem. Eng. (2018) .
[8] Curto, D., Franzitta, V., and Guercio, A., Appl. Sci. vol **11**, issue 2 (2021) pp.1–36.
[9] Yalcinkaya, F., J. Eng. Fiber. Fabr. vol **14** (2019) .
[10] Singh, A., Sharma, M., and Singh, I., Proc. Inst. Mech. Eng. Part B J. Eng. Manuf. vol **231**, issue 13 (2016) pp.0954405416629864–2407.
[11] Damtie, M. M., Kim, B., Woo, Y. C., and Choi, J. S., Chemosphere (2018) .
[12] Seo, D. H., Pineda, S., Woo, Y. C., Xie, M., Murdock, A. T., Ang, E. Y. M., Jiao, Y., Park, M. J., Lim, S. Il, Lawn, M., Borghi, F. F., Han, Z. J., Gray, S., Millar, G., Du, A., Shon, H. K., Ng, T. Y., and Ostrikov, K., Nat. Commun. (2018) .
[13] Warsinger, D. M., Tow, E. W., Swaminathan, J., and Lienhard V, J. H., J. Memb. Sci. (2017) .
[14] Deshmukh, A., Boo, C., Karanikola, V., Lin, S., Straub, A. P., Tong, T., Warsinger, D. M., and Elimelech, M., Energy Environ. Sci. (2018) .
[15] Warsinger, D. M., Servi, A., Connors, G. B., Mavukkandy, M. O., Arafat, H. A., Gleason, K. K., and Lienhard, J. H., Environ. Sci. Water Res. Technol. vol **3**, issue 5 (2017) pp.930–939.
[16] Rezaei, M., Warsinger, D. M., Lienhard V, J. H., Duke, M. C., Matsuura, T., and Samhaber, W. M., Water Res. (2018) .
[17] Shi, X., Zhou, W., Ma, D., Ma, Q., and Bridges, D., J. Nanomater. vol **2015**, issue May (2015) .
[18] Wang, Z., Hao, L., Yang, F., and Wei, Q., Membranes (Basel). vol **10**, issue 4 (2020) .
[19] Guo, J., Deka, B. J., Kim, K. J., and An, A. K., Desalination (2019) .
[20] Zhang, R., Tang, W., Gao, H., Wu, C., Gray, S., and Lu, X., Sep. Purif. Technol. (2020) p.117762.
[21] Chen, J., Han, J., and Xu, D., Mater. Lett. vol **246** (2019) pp.20–23.
[22] Liang, W., Chenyang, Y., Bin, Z., Xiaona, W., Zijun, Y., Lixiang, Z., Hongwei, Z., and Nanwen, L., J. Memb. Sci. vol **569** (2019) pp.157–165.
[23] Ahmadi, Z., Ravandi, S. A. H., Haghighat, F., and Dabirian, F., Fibers Polym. vol **21**, issue 6 (2020) pp.1200–1211.
[24] Ryšánek, P., Benada, O., Tokarský, J., Syrový, M., Čapková, P., and Pavlík, J., Mater. Sci. Eng.

C vol **105**, issue June (2019) .
[25] Chaúque, E. F. C., Dlamini, L. N., Adelodun, A. A., Greyling, C. J., and Ngila, J. C., Phys. Chem. Earth vol **100** (2017) pp.201–211.
[26] Hong, G., Li, X., Shen, L., Wang, M., Wang, C., Yu, X., and Wang, X., J. Hazard. Mater. vol **295** (2015) pp.161–169.
[27] Kampalanonwat, P., and Supaphol, P., Energy Procedia vol **56**, issue C (2014) pp.142–151.
[28] Wu, H., Shen, F., Su, Y., Chen, X., and Wan, Y., Sep. Purif. Technol. vol **197**, issue March 2017 (2018) pp.178–188.
[29] Seo, D. H., Pineda, S., Woo, Y. C., Xie, M., Murdock, A. T., Ang, E. Y. M., Jiao, Y., Park, M. J., Lim, S. Il, Lawn, M., Borghi, F. F., Han, Z. J., Gray, S., Millar, G., Du, A., Shon, H. K., Ng, T. Y., and Ostrikov, K., Nat. Commun. vol **9**, issue 1 (2018) pp.1–12.
[30] Fang, J., Wang, H., Wang, X., and Lin, T., J. Text. Inst. vol **103**, issue 9 (2012) pp.937–944.
[31] Liu, L., Shen, F., Chen, X., Luo, J., Su, Y., Wu, H., and Wan, Y., J. Memb. Sci. vol **499** (2016) pp.544–554.
[32] Ebrahimi, F., Orooji, Y., and Razmjou, A., Polymers (Basel). (2020) .
[33] Alghoraibi, I., and Alomari, S., *Different Methods for Nanofiber Design and Fabrication*.
[34] Bortolassi, A. C. C., Nagarajan, S., de Araújo Lima, B., Guerra, V. G., Aguiar, M. L., Huon, V., Soussan, L., Cornu, D., Miele, P., and Bechelany, M., Mater. Sci. Eng. C vol **102** (2019) pp.718–729.
[35] Nurfaizey, A., Roslan, N., Hafiz, M., Rosli, M., Saad, A., and Tucker, N., J. Adv. Manuf. Technol. vol **14**, issue 2(1) (2020) pp.91–100.
[36] Ren, L. F., Xia, F., Shao, J., Zhang, X., and Li, J., Desalination (2017) .
[37] Meyva-Zeybek, Y., and Kaynak, C., J. Appl. Polym. Sci. vol **138**, issue 3 (2021) pp.1–11.
[38] Munajat, N. A., Nurfaizey, A. H., Husin, M. H. M., Siti Hajar, S. H. S., Omar, G., and Salim, M. A., J. Adv. Res. Fluid Mech. Therm. Sci. vol **49**, issue 2 (2018) pp.85–91.
[39] Essalhi, M., Khayet, M., Tesfalidet, S., Alsultan, M., and Tavajohi, N., Chem. Eng. J. vol **426**, issue April (2021) p.131316.
[40] Wang, R., Liu, Y., Li, B., Hsiao, B. S., and Chu, B., J. Memb. Sci. vol **392–393** (2012) pp.167–174.
[41] Islam, M. S., Ang, B. C., Andriyana, A., and Afifi, A. M., SN Appl. Sci. vol **1**, issue 10 (2019) .
[42] Nonato, R. C., Morales, A. R., Rocha, M. C., Nista, S. V. G., Mei, L. H. I., and Bonse, B. C., Appl. Phys. A Mater. Sci. Process. vol **123**, issue 1 (2017) pp.1–8.
[43] Nurfaizey, A. H., Akop, M. Z., Salim, M. A., Mohd Rosli, M. A., and Masripan, N. A., World J. Eng. vol **17**, issue 1 (2020) pp.52–59.
[44] Su, Z., Ding, J., and Wei, G., RSC Adv. vol **4**, issue 94 (2014) pp.52598–52610.
[45] Tucker, N., Stanger, J. J., Staiger, M. P., Razzaq, H., and Hofman, K., J. Eng. Fiber. Fabr. vol **7**, issue 3 (2012) pp.63–73.
[46] Haider, A., Haider, S., and Kang, I. K., Arab. J. Chem. vol **11**, issue 8 (2018) pp.1165–1188.
[47] Zhu, Z., Zhong, L., Horseman, T., Liu, Z., Zeng, G., Li, Z., Lin, S., and Wang, W., J. Memb. Sci., issue June (2020) p.118768.
[48] Maleki, M., Latifi, M., and Amani-Tehran, M., World Acad. Sci. Eng. Technol. vol **64** (2010) pp.389–392.
[49] Nurfaizey, A. H., Long, F. C., Daud, M. A. M., Muhammad, N., Mansor, M. R., and Tucker, N., J. Mech. Eng. Sci. vol **13**, issue 1 (2019) pp.4679–4692.
[50] Nurfaizey, A. H., Salim, M. A., Tamaldin, N., Nadlene, R., Kamarolzaman, A. A., and Tucker, N., Int. J. Nanoelectron. Mater. vol **13**, issue Special Issue ISSTE2019 (2020) pp.177–186.
[51] Wang, T., and Kumar, S., J. Appl. Polym. Sci. vol **102**, issue 2 (2006) pp.1023–1029.
[52] Ahmed, F. E., Lalia, B. S., and Hashaikeh, R., Desalination vol **356** (2015) pp.15–30.
[53] Li, Z., and Wang, C., One-Dimensional Nanostructures (2013) pp.15–28.
[54] Rivero, P. J., Redin, D. M., and Rodríguez, R. J., Metals (Basel). vol **10**, issue 3 (2020) .
[55] Stachewicz, U., Dijksman, J. F., Soudani, C., Tunnicliffe, L. B., Busfield, J. J. C., and Barber, A. H., Eur. Polym. J. vol **91**, issue January (2017) pp.368–375.
[56] Moghadam, B. H., and Hasanzadeh, M., Adv. Polym. Technol. (2013) .
[57] Ahire, J. J., Neveling, D. P., and Dicks, L. M. T., Appl. Microbiol. Biotechnol. vol **102**, issue 16

(2018) pp.7171–7181.
[58] Kim, S. C., Kang, S., Lee, H., Kwak, D. Bin, Ou, Q., Pei, C., and Pui, D. Y. H., Aerosol Air Qual. Res. (2020) .
[59] Aman Mohammadi, M., Hosseini, S. M., and Yousefi, M., Food Sci. Nutr. vol **8**, issue 9 (2020) pp.4656–4665.
[60] Can-Herrera, L. A., Oliva, A. I., Dzul-Cervantes, M. A. A., Pacheco-Salazar, O. F., and Cervantes-Uc, J. M., Polymers (Basel). vol **13**, issue 4 (2021) pp.1–16.
[61] Khan, Z., Kafiah, F., Zahid Shafi, H., Nufaiei, F., Ahmed Furquan, S., and Matin, A., Int. J. Adv. Eng. Nano Technol., issue 3 (2015) pp.2347–6389.
[62] Borhani, S., Asadi, A., and Dabbagh, H. A., J. Water Health vol **18**, issue 2 (2020) pp.106–117.
[63] Barua, B., and Saha, M. C., J. Appl. Polym. Sci. (2015) .
[64] Bakar, S. S. S., Fong, K. C., Eleyas, A., and Nazeri, M. F. M., IOP Conf. Ser. Mater. Sci. Eng. vol **318**, issue 1 (2018) .
[65] Ramesh Kumar, P., Khan, N., Vivekanandhan, S., Satyanarayana, N., Mohanty, A. K., and Misra, M., *Journal of Nanoscience and Nanotechnology*.
[66] Levitt, A. S., Vallett, R., Dion, G., and Schauer, C. L., J. Appl. Polym. Sci. vol **135**, issue 25 (2018) pp.1–9.
[67] Matabola, K. P., and Moutloali, R. M., J. Mater. Sci. vol **48**, issue 16 (2013) pp.5475–5482.
[68] Hekmati, A. H., Rashidi, A., Ghazisaeidi, R., and Drean, J. Y., Text. Res. J. vol **83**, issue 14 (2013) pp.1452–1466.
[69] Yördem, O. S., Papila, M., and Menceloğlu, Y. Z., Mater. Des. vol **29**, issue 1 (2008) pp.34–44.
[70] Nurfaizey, A. H., and Munajat, N. A., , issue December (2020) pp.94–96.
[71] Danny Pratama Lamura, M., Pulungan, M. A., Jauhari, J., and Sriyanti, I., IOP Conf. Ser. Earth Environ. Sci. vol **1796**, issue 1 (2021) .
[72] Yuan, X. Y., Zhang, Y. Y., Dong, C., and Sheng, J., Polym. Int. vol **53**, issue 11 (2004) pp.1704–1710.
[73] Nurfaizey, A., Long, F., Daud, M., Masripan, N., and Tucker, N., J. Adv. Manuf. Technol. vol **14**, issue 2(1) (2020) pp.1–11.
[74] Zargham, S., Bazgir, S., Tavakoli, A., Rashidi, A. S., and Damerchely, R., J. Eng. Fiber. Fabr. vol **7**, issue 4 (2012) pp.42–49.
[75] Daemi, H., Mashayekhi, M., and Pezeshki Modaress, M., Carbohydr. Polym. vol **198**, issue May (2018) pp.481–485.
[76] Tang, X. P., Si, N., Xu, L., and Liu, H. Y., Therm. Sci. vol **18**, issue 5 (2014) pp.1447–1449.
[77] Zhang, C., Yuan, X., Wu, L., Han, Y., and Sheng, J., Eur. Polym. J. vol **41**, issue 3 (2005) pp.423–432.
[78] Rafizadeh, M., Fallahi, D., Mohammadi, N., and Vahidi, B., E-Polymers, issue January (2009) .
[79] Selatile, M. K., Ray, S. S., Ojijo, V., and Sadiku, R., Fibers Polym. vol **20**, issue 1 (2019) pp.100–112.
[80] Veeramuthu, L., Venkatesan, M., Liang, F. C., Benas, J. S., Cho, C. J., Chen, C. W., Zhou, Y., Lee, R. H., and Kuo, C. C., Polymers (Basel). vol **12**, issue 3 (2020) pp.1–28.
[81] Huan, S., Liu, G., Han, G., Cheng, W., Fu, Z., Wu, Q., and Wang, Q., Materials (Basel). vol **8**, issue 5 (2015) pp.2718–2734.
[82] Yang, G. Z., Li, H. P., Yang, J. H., Wan, J., and Yu, D. G., Nanoscale Res. Lett. vol **12**, issue 1 (2017) .
[83] Szewczyk, P. K., and Stachewicz, U., Adv. Colloid Interface Sci. vol **286** (2020) p.102315.
[84] Barua, B., and Mrinal, C. S., Polym. Eng. Sci. (2017) pp.1–10.
[85] Nezarati, R. M., Eifert, M. B., and Cosgriff-Hernandez, E., Tissue Eng. - Part C Methods vol **19**, issue 10 (2013) pp.810–819.
[86] De Vrieze, S., Van Camp, T., Nelvig, A., Hagström, B., Westbroek, P., and De Clerck, K., J. Mater. Sci. vol **44**, issue 5 (2009) pp.1357–1362.
[87] Santos de Oliveira Junior, M., Manzolli Rodrigues, B. V., Marcuzzo, J. S., Guerrini, L. M.,

Baldan, M. R., and Rezende, M. C., J. Appl. Polym. Sci. vol **134**, issue 43 (2017) pp.1–10.
[88] Lee, J., Yoon, J., Kim, J. H., Lee, T., and Byun, H., J. Appl. Polym. Sci. vol **135**, issue 7 (2018) pp.1–9.
[89] Wang, W., Zheng, Y., Jin, X., Sun, Y., Lu, B., Wang, H., Fang, J., Shao, H., and Lin, T., Nano Energy (2019) .
[90] Zaca-Moran, O., Sánchez-Ramírez, J. F., Herrera-Pérez, J. L., and Díaz-Reyes, J., Mater. Sci. Semicond. Process. vol **127**, issue January (2021) .
[91] Niu, Z., Bian, Y., Xia, T., Zhang, L., and Chen, C., Build. Environ. vol **188**, issue November 2020 (2021) p.107449.
[92] Kusuma, N. C., Purwanto, M., Sudrajat, M. A., Jaafar, J., Othman, M. H. D., Aziz, M. H. A., Raharjo, Y., and Qtaishat, M. R., J. Environ. Chem. Eng. vol **9**, issue 4 (2021) p.105582.
[93] Liao, Y., Zheng, G., Huang, J. J., Tian, M., and Wang, R., J. Memb. Sci. (2020) .
[94] Dong, S., Yun, Y., Wang, M., Li, C., Fu, H., Li, X., Yang, W., and Liu, G., J. Taiwan Inst. Chem. Eng. (2020) .
[95] Deka, B. J., Lee, E. J., Guo, J., Kharraz, J., and An, A. K., Environ. Sci. Technol. vol **53**, issue 9 (2019) pp.4948–4958.
[96] Niknejad, A. S., Bazgir, S., Kargari, A., Barani, M., Ranjbari, E., and Rasouli, M., J. Memb. Sci. vol **638**, issue August (2021) p.119744.
[97] Zhang, Z., Xu, S., Wu, Y., Shi, S., and Xiao, G., Membranes (Basel). vol **11**, issue 6 (2021) .
[98] Thi Tra My, N., Thi Yen Nhi, V., and Xuan Thanh, B., J. Appl. Membr. Sci. Technol. vol **22**, issue 1 (2018) .
[99] Zhu, Z., Zhong, L., Horseman, T., Liu, Z., Zeng, G., Li, Z., Lin, S., and Wang, W., J. Memb. Sci. vol **620** (2021) pp.1–9.
[100] Jiang, S., Chen, Y., Duan, G., Mei, C., Greiner, A., and Agarwal, S., Polym. Chem. vol **9**, issue 20 (2018) pp.2685–2720.
[101] Ademola Bode-Aluko, C., Pereao, O., Kyaw, H. H., Al-Naamani, L., Al-Abri, M. Z., Tay Zar Myint, M., Rossouw, A., Fatoba, O., Petrik, L., and Dobretsov, S., Mater. Sci. Eng. B Solid-State Mater. Adv. Technol. vol **264**, issue February 2020 (2021) p.114913.
[102] Ismar, E., and Sarac, A. S., Polym. Bull. vol **75**, issue 2 (2018) pp.485–499.
[103] Arifeen, W. U., Kim, M., Choi, J., Yoo, K., Kurniawan, R., and Ko, T. J., Mater. Chem. Phys. vol **229**, issue February (2019) pp.310–318.
[104] Celep, G. K., and Dincer, K., Int. Polym. Process. vol **32**, issue 4 (2017) pp.508–514.
[105] Ma, H., and Hsiao, B. S., *Electrospun Nanofibrous Membranes for Desalination*, Elsevier Inc.
[106] Muhamad, N. A. S., Mokhtar, N. M., Naim, R., Lau, W. J., and Ismail, A. F., Int. J. Eng. Technol. Sci. vol **6**, issue June (2019) pp.62–81.
[107] Khalifa, A., Ahmad, H., Antar, M., Laoui, T., and Khayet, M., Desalination vol **404** (2017) pp.22–34.
[108] Roche, R., and Yalcinkaya, F., ChemistryOpen vol **8**, issue 1 (2019) pp.97–103.
[109] Jasmee, S., Omar, G., Masripan, N. A. B., Kamarolzaman, A. A., Ashikin, A. S., and Che Ani, F., Mater. Res. Express vol **5**, issue 9 (2018) .
[110] Seyed Shahabadi, S. M., Rabiee, H., Seyedi, S. M., Mokhtare, A., and Brant, J. A., J. Memb. Sci. vol **537**, issue October (2017) pp.140–150.
[111] Nguyen-Tri, P., Tran, H. N., Plamondon, C. O., Tuduri, L., Vo, D. V. N., Nanda, S., Mishra, A., Chao, H. P., and Bajpai, A. K., Prog. Org. Coatings vol **132**, issue January (2019) pp.235–256.
[112] Shao, Y., Han, M., Wang, Y., Li, G., Xiao, W., Li, X., Wu, X., Ruan, X., Yan, X., He, G., and Jiang, X., J. Memb. Sci. vol **579**, issue February (2019) pp.240–252.
[113] Uddin, M. N., Desai, F. J., Rahman, M. M., and Asmatulu, R., Nanoscale Adv. (2020) .
[114] Akkaya, A., and Ozseker, E. E., Polym. Test. vol **78**, issue March (2019) p.105959.
[115] Haider, M. K., Ullah, A., Sarwar, M. N., Yamaguchi, T., Wang, Q., Ullah, S., Park, S., and Kim, I. S., Polymers (Basel). vol **13**, issue 5 (2021) pp.1–20.
[116] Yu, Y., Zhang, F., Liu, Y., Zheng, Y., Xin, B., Jiang, Z., Peng, X., and Jin, S., J. Mater. Res. vol **35**, issue 9 (2020) pp.1173–1181.
[117] Szewczyk, P. K., Ura, D. P., Metwally, S., Knapczyk-Korczak, J., Gajek, M., Marzec, M. M.,

Bernasik, A., and Stachewicz, U., Polymers (Basel). vol **11**, issue 1 (2018) .
[118] Heshmati, M. R., Amiri, S., and Hosseini-Zori, M., Open J. Org. Polym. Mater. vol **10**, issue 01 (2020) pp.1–15.
[119] Iacono, S. T., and Jennings, A. R., Nanomaterials vol **9**, issue 684 (2019) pp.1–18.
[120] Nuraje, N., Khan, W. S., Lei, Y., Ceylan, M., and Asmatulu, R., J. Mater. Chem. A vol **1**, issue 6 (2013) pp.1929–1946.
[121] Almasian, A., Chizari Fard, G., Mirjalili, M., and Parvinzadeh Gashti, M., J. Ind. Eng. Chem. vol **62** (2018) pp.146–155.
[122] Rostami, A., Pirsaheb, M., Moradi, G., and Derakhshan, A. A., Polym. Adv. Technol. vol **31**, issue 5 (2020) pp.941–956.
[123] Sheng, J., Xu, Y., Yu, J., and Ding, B., ACS Appl. Mater. Interfaces vol **9**, issue 17 (2017) pp.15139–15147.
[124] Cai, Y., Xu, X., Wei, Q., Ke, H., Yao, W., Qiao, H., Lai, C., He, G., Zhao, Y., and Fong, H., E-Polymers, issue 018 (2012) pp.1–10.
[125] Alarifi, I. M., Khan, W. S., and Asmatulu, R., PLoS One vol **13**, issue 8 (2018) pp.1–14.
[126] Khan, W. S., Ceylan, M., Jabarrania, A., Saeednia, L., and Asmatulu, R., J. Therm. Eng. vol **3**, issue 4 (2017) pp.1375–1390.
[127] Gu, S., Cai, R., and Yan, Y., Chem. Commun. vol **47**, issue 10 (2011) pp.2856–2858.
[128] Mapazi, O., Matabola, K. P., Moutloali, R. M., and Ngila, C. J., Polymer (Guildf). vol **149** (2018) pp.106–116.
[129] Khayyam, H., Jazar, R. N., Nunna, S., Golkarnarenji, G., Badii, K., Fakhrhoseini, S. M., Kumar, S., and Naebe, M., Prog. Mater. Sci. vol **107**, issue April 2018 (2020) p.100575.
[130] Nataraj, S. K., Yang, K. S., and Aminabhavi, T. M., Prog. Polym. Sci. vol **37**, issue 3 (2012) pp.487–513.
[131] Li, W., Yang, Z., Meng, Q., Shen, C., and Zhang, G., J. Memb. Sci. vol **467** (2014) pp.253–261.
[132] Alarifi, I. M., Alharbi, A., Khan, W. S., Swindle, A., and Asmatulu, R., Materials (Basel). vol **8**, issue 10 (2015) pp.7017–7031.
[133] Furushima, Y., Nakada, M., Takahashi, H., and Ishikiriyama, K., Polymer (Guildf). vol **55**, issue 13 (2014) pp.3075–3081.
[134] Szepcsik, B., and Pukánszky, B., Thermochim. Acta vol **671**, issue December 2018 (2019) pp.200–208.
[135] Rahaman, M. S. A., Ismail, A. F., and Mustafa, A., Polym. Degrad. Stab. vol **92**, issue 8 (2007) pp.1421–1432.
[136] Dalton, S., Heatley, F., and Budd, P. M., Polymer (Guildf). vol **40**, issue 20 (1999) pp.5531–5543.
[137] Furushima, Y., Kumazawa, R., Yamaguchi, Y., Hirota, N., Sawada, K., Nakada, M., and Murakami, M., Polymer (Guildf). vol **226**, issue January (2021) p.123780.
[138] Qiao, M., Kong, H., Ding, X., Hu, Z., Zhang, L., Cao, Y., and Yu, M., Polymers (Basel). vol **11**, issue 3 (2019) .
[139] Konstantopoulos, G., Soulis, S., Dragatogiannis, D., and Charitidis, C., Materials (Basel). vol **13**, issue 12 (2020) pp.1–26.
[140] Soulis, S., Dragatogiannis, D. A., and Charitidis, C. A., Polym. Adv. Technol. vol **31**, issue 6 (2020) pp.1403–1413.
[141] Liu, Y., and Kumar, S., Polym. Rev. vol **52**, issue 3–4 (2012) pp.234–258.
[142] Munajat, N. A., Nurfaizey, A. H., Bahar, A. A. M., You, K. Y., Fadzullah, S. H. S. M., and Omar, G., Microw. Opt. Technol. Lett. vol **60**, issue 9 (2018) pp.2198–2204.
[143] Wu, S., Zhang, F., Yu, Y., Li, P., Yang, X., Lu, J., and Ryu, S., Compos. Interfaces vol **15**, issue 7–9 (2008) pp.671–677.
[144] Maghe, M., Creighton, C., Henderson, L. C., Huson, M. G., Nunna, S., Atkiss, S., Byrne, N., and Fox, B. L., J. Mater. Chem. A vol **4**, issue 42 (2016) pp.16619–16626.
[145] Wu, M., Wang, Q., Li, K., Wu, Y., and Liu, H., Polym. Degrad. Stab. vol **97**, issue 8 (2012) pp.1511–1519.
[146] Altaleb, H. A., Thamer, B. M., Abdulhameed, M. M., El-Hamshary, H., Mohammady, S. Z., and Al-Enizi, A. M., J. Environ. Chem. Eng. vol **9**, issue 4 (2021) p.105361.

[147] Tao, D., Li, X., Dong, Y., Zhu, Y., Yuan, Y., Ni, Q., Fu, Y., and Fu, S., Compos. Sci. Technol. vol **188**, issue November 2019 (2020) p.107992.
[148] Freitas, S. K. S., Borges, R. S., Merlini, C., Barra, G. M. O., and Esteves, P. M., J. Phys. Chem. C vol **121**, issue 48 (2017) pp.27247–27252.
[149] Hamadneh, N. N., Khan, W. S., and Khan, W. A., J. King Saud Univ. - Sci. vol **31**, issue 4 (2019) pp.618–627.
[150] Karim, S. A., Mohamed, A., Abdel-Mottaleb, M. M., Osman, T. A., and Khattab, A., Arab. J. Sci. Eng. vol **43**, issue 9 (2018) pp.4697–4702.
[151] Duan, G., Zhang, H., Jiang, S., Xie, M., Peng, X., Chen, S., Hanif, M., and Hou, H., Mater. Lett. vol **122** (2014) pp.178–181.
[152] Youm, J. S., Kim, J. H., Kim, C. H., Kim, J. C., Kim, Y. A., and Yang, K. S., J. Appl. Polym. Sci. vol **133**, issue 37 (2016) pp.1–9.
[153] Lai, C., Zhong, G., Yue, Z., Chen, G., Zhang, L., Vakili, A., Wang, Y., Zhu, L., Liu, J., and Fong, H., Polymer (Guildf). vol **52**, issue 2 (2011) pp.519–528.
[154] Liu, S. D., Li, D. Sen, Yang, Y., and Jiang, L., Nanotechnol. Rev. vol **8**, issue 1 (2019) pp.218–226.
[155] Balan, K. K., Sivanesan, V., Moorthy, N., Budhhan, D., Jeyaseelan, S., and Sundaramoorthy, S., Mater. Today Proc. vol **3**, issue 6 (2016) pp.1320–1329.
[156] Wong, S. C., Baji, A., and Leng, S., Polymer (Guildf). vol **49**, issue 21 (2008) pp.4713–4722.
[157] Song, K., Zhang, Y., Meng, J., Green, E. C., Tajaddod, N., Li, H., and Minus, M. L., Materials (Basel). vol **6**, issue 6 (2013) pp.2543–2577.
[158] Eren, O., Ucar, N., Onen, A., Kızıldag, N., Vurur, O. F., Demirsoy, N., and Karacan, I., Int. J. Chem. Mol. Nucl. Mater. Metall. Eng. vol **8**, issue 8 (2014) pp.726–728.
[159] Du, L., Quan, X., Fan, X., Wei, G., and Chen, S., J. Memb. Sci. vol **596**, issue October 2019 (2020) p.117613.
[160] Duan, Q., Wang, B., and Wang, H., J. Macromol. Sci. Part B Phys. vol **51**, issue 12 (2012) pp.2428–2437.
[161] Lee, S., Kim, J., Ku, B.-C., Kim, J., and Joh, H.-I., Adv. Chem. Eng. Sci. vol **02**, issue 02 (2012) pp.275–282.
[162] El-Hadi, A. M., Mohan, S. D., Davis, F. J., and Mitchell, G. R., J. Polym. Res. vol **21**, issue 12 (2014) .
[163] Arif, M. W. A., Nurfaizey, A. H., Mustafa, Z., Nadlene, R., Jaafar, J., and Tucker, N., Int. J. Nanoelectron. Mater. vol **14**, issue August (2021) pp.213–224.
[164] Arifeen, W. U., Kim, M., Choi, J., Yoo, K., Kurniawan, R., and Ko, T. J., Mater. Chem. Phys. (2019) .
[165] Ali, A., Quist-Jensen, C. A., Macedonio, F., and Drioli, E., J. Membr. Sci. Res. vol **2** (2016) pp.179–185.
[166] Eykens, L., De Sitter, K., Dotremont, C., Pinoy, L., and Van der Bruggen, B., Sep. Purif. Technol. vol **182** (2017) pp.36–51.
[167] Wang, P., and Chung, T. S., J. Memb. Sci. vol **474** (2015) pp.39–56.
[168] Tijing, L. D., Woo, Y. C., Choi, J. S., Lee, S., Kim, S. H., and Shon, H. K., J. Memb. Sci. vol **475** (2015) pp.215–244.
[169] Kang, G. dong, and Cao, Y. ming, J. Memb. Sci. vol **463** (2014) pp.145–165.
[170] Nthunya, L. N., Gutierrez, L., Verliefde, A. R., and Mhlanga, S. D., J. Chem. Technol. Biotechnol. vol **94**, issue 9 (2019) pp.2826–2837.
[171] Nthunya, L. N., Gutierrez, L., Derese, S., Mamba, B. B., Verliefde, A. R., and Mhlanga, S. D., J. Environ. Chem. Eng. vol **7**, issue 4 (2019) p.103254.
[172] Huang, A., and Feng, B., J. Memb. Sci. vol **548**, issue October 2017 (2018) pp.59–65.
[173] Cai, J., Liu, Z., and Guo, F., Membranes (Basel). vol **11**, issue 1 (2021) pp.1–14.
[174] Woo, Y. C., Tijing, L. D., Park, M. J., Yao, M., Choi, J. S., Lee, S., Kim, S. H., An, K. J., and Shon, H. K., Desalination vol **403** (2017) pp.187–198.
[175] Tijing, L. D., Woo, Y. C., Johir, M. A. H., Choi, J. S., and Shon, H. K., Chem. Eng. J. vol **256** (2014) pp.155–159.
[176] Efome, J. E., Rana, D., Matsuura, T., Yang, F., Cong, Y., and Lan, C. Q., ACS Sustain. Chem. Eng.

vol **8**, issue 17 (2020) pp.6601–6610.
[177] Li, X., Deng, L., Yu, X., Wang, M., Wang, X., García-Payo, C., and Khayet, M., J. Mater. Chem. A vol **4**, issue 37 (2016) pp.14453–14463.
[178] Tang, M., Hou, D., Ding, C., Wang, K., Wang, D., and Wang, J., Sci. Total Environ. vol **696** (2019) p.133883.
[179] Qin, D., Zhang, R., Cao, B., and Li, P., J. Memb. Sci. vol **638**, issue July (2021) p.119672.
[180] Cai, J., Liu, X., Zhao, Y., and Guo, F., Desalination vol **429**, issue August 2017 (2018) pp.70–75.